



Contents lists available at SciVerse ScienceDirect

Journal of Computational and Applied Mathematics

journal homepage: www.elsevier.com/locate/cam

On micromechanical damage modeling in geomechanics: Influence of numerical integration scheme

S. Levasseur^{a,c,*}, F. Collin^a, R. Charlier^a, D. Kondo^b^a Université de Liège, Chemin des chevreuils 1, B-4000 Liège 1, Belgium^b Institut d'Alembert, Université Pierre et Marie Curie, 4 place Jussieu, F-75005 Paris, France^c FRS-FNRS, 5 rue d'Egmont, B-1000 Bruxelles, Belgium

ARTICLE INFO

Article history:

Received 31 January 2012

Received in revised form 30 April 2012

Keywords:

Anisotropic damage

Initial stresses

Micromechanics

Microcracked geomaterials

Tunnel excavation

Numerical integration

ABSTRACT

Tunnel excavations in deep rocks provide stress perturbations which initiate diffuse and/or localized damage propagation in the material. This damage phenomenon can lead to significant irreversible deformations and changes in rock properties. In this paper, we propose to model such behavior by considering a micromechanically-based damage approach. The resulting micromechanical model, which also accounts for initial stress, is described and assessed through the numerical analysis of a synthetic tunnel drilling in Opalinus Clay. A particular emphasis is put on the numerical integration of the model. In particular, an appropriate choice of the latter is required to ensure the numerical stability and a confident prediction of excavation damaged zone around tunnels.

© 2012 Elsevier B.V. All rights reserved.

1. Introduction

A zone with significant irreversible deformations and significant changes in flow and transport properties (named the *Excavation Damaged Zone* or EDZ) is expected to be formed around underground excavations in deep geological layers considered for high level radioactive waste disposal. Stress perturbations generated around the excavation could lead to a significant change of the hydromechanical properties, due to diffuse and/or localized microcrack propagation in the material [1]. The modeling of such behavior is classically performed by considering macroscopic damage models (see among others [2]). Recent developments in the field of homogenization methods provide a physically and mathematically appropriate framework for the investigation of the behavior of microcracked media including the description of anisotropic induced damage, as well as crack closure effects [3–5]. In the perspective of applications to civil engineering and geotechnical problems, such as underground excavations, it is desirable to assess the various available homogenization schemes through the analysis of their capability to solve these problems. To this end, numerical investigation of responses predicted by these micromechanical models at the material level as well as for geostructures is due. The purpose of this study is then to present an analysis of a micromechanical damage approach in order to provide an appropriate interpretation of the nonlinear behavior of underground structures. To do this, a general micro–macro model including damage-induced anisotropy, microcrack closure effects and initial stress is exposed in Section 2. This model generalizes the one recently proposed [6–8] to an overall formulation for dilute, Mori–Tanaka and Ponte-Castaneda and Willis homogenization schemes. In Section 3, we then present an application consisting of the modeling of a synthetic tunnel excavation in clayey rocks. This application, inspired from the SELFRAC dilatometer test experiment [1] performed in Opalinus Clay, allows us to propose a characterization of the excavation damaged zone around a tunnel and an assessment of the proposed model. This application

* Corresponding author at: Université de Liège, Chemin des chevreuils 1, B-4000 Liège 1, Belgium.

E-mail address: severine.levasseur@ulg.ac.be (S. Levasseur).

also demonstrates the need to carefully choose the numerical integration scheme of the micromechanical damage model in the context of large scale structural problem modeling.

2. Micromechanical modeling of damage

2.1. Principle

The proposed micromechanical modeling including initial stresses is first based on a representative elementary volume (*rev*, Ω) made up of a solid matrix s (occupying a domain Ω^s) and an arbitrary system of penny-shaped microcracks. Each microcrack family is denoted r and occupies a domain Ω^r . The matrix behavior is supposed elastic whereas an initial uniform stress field σ_0 is assumed in the solid matrix occupying a domain Ω^s . The local constitutive equations in the heterogeneous medium with prestress are then:

$$(\underline{z} \in \Omega) \quad \sigma(\underline{z}) = \mathbb{C}(\underline{z}) : \epsilon(\underline{z}) + \sigma^p(\underline{z}) \quad (1)$$

where $\sigma(\underline{z})$ denotes the local stress tensor, $\mathbb{C}(\underline{z})$ represents the heterogeneous stiffness tensor and $\sigma^p(\underline{z})$ corresponds to a prestress tensor such as:

$$\mathbb{C}(\underline{z}) = \begin{cases} \mathbb{C}^s & \text{in } (\Omega^s) \\ \mathbf{0} & \text{in } (\Omega^r) \end{cases} \quad \sigma^p(\underline{z}) = \begin{cases} \sigma_0 & \text{in } (\Omega^s) \\ \mathbf{0} & \text{in } (\Omega^r) \end{cases} \quad (2)$$

for which it is recalled that Ω^s and Ω^r represent respectively the domain occupied by the matrix and by cracks.

Following [7,8], this problem can be solved by using the classical Levin theorem [9,10], from which the overall energy potential and the first state law are deduced as follow:

$$\Psi = \left(\frac{1}{2} \mathbf{E} : \mathbb{C}^s + \sigma_0 \right) : \left(\mathbb{I} - \sum_{r=1}^N \varphi^r \mathbb{A}^r \right) : \mathbf{E} = \left(\frac{1}{2} \mathbf{E} + \sigma_0 : \mathbb{C}^{s-1} \right) : \mathbb{C}^{hom} : \mathbf{E} \quad (3)$$

$$\Sigma = (\mathbb{C}^s : \mathbf{E} + \sigma_0) : \left(\mathbb{I} - \sum_{r=1}^N \varphi^r \mathbb{A}^r \right) \quad (4)$$

where Σ and \mathbf{E} are respectively the macroscopic stress and strain tensors and φ^r represents the volume fraction of the r microcrack family. The corresponding microcrack density d^r is related to φ^r by: $\varphi^r = \frac{4\pi}{3} w_r d^r$, in which w_r is the microcrack aspect ratio. The 4th-order tensor \mathbb{A}^r represents the average value of the localization tensor of the r th crack family. The resulting homogenized stiffness tensor \mathbb{C}^{hom} reads:

$$\mathbb{C}^{hom} = \mathbb{C}^s : \left(\mathbb{I} - \frac{4\pi}{3} \sum_{r=1}^N w_r d^r \mathbb{A}^r \right). \quad (5)$$

The localization tensor, \mathbb{A}^r , depends on the considered homogenization scheme (see [11–13]).

- In the case of the dilute approximation:

$$\mathbb{A}_{dil}^r = (\mathbb{I} - \mathbb{S}^r)^{-1}. \quad (6)$$

- For the Mori–Tanaka approximation:

$$\mathbb{A}_{MT}^r = (\mathbb{I} - \mathbb{S}^r)^{-1} : \left[\mathbb{I} + \frac{4\pi}{3} \sum_{j=1}^N w_j d^j (\mathbb{I} - \mathbb{S}^j)^{-1} \right]^{-1}. \quad (7)$$

- In the case of Ponte-Castaneda and Willis (PCW) bounds:

$$\mathbb{A}_{PCW}^r = (\mathbb{I} - \mathbb{S}^r)^{-1} : \left[\mathbb{I} + \frac{4\pi}{3} \sum_{j=1}^N w_j d^j (\mathbb{I} - \mathbb{S}^j + \mathbb{S}_d) : (\mathbb{I} - \mathbb{S}^j)^{-1} \right]^{-1} \quad (8)$$

in which \mathbb{S}^r is the Eshelby tensor, whose expression for penny-shaped cracks can be found in [12], and \mathbb{S}_d describes the spatial distribution of microcracks (see [13]). Note that for a spherical spatial distribution of microcracks (PCW bounds) \mathbb{S}_d is given by the isotropic tensor:

$$\mathbb{S}_d = \alpha \mathbb{J} + \beta \mathbb{K} \quad \text{with } \alpha = \frac{3k^s}{3k^s + 4\mu^s} \quad \text{and} \quad \beta = \frac{6(k^s + 2\mu^s)}{5(3k^s + 4\mu^s)}.$$

Furthermore, for one single crack family, if $\mathbb{S}_d = \mathbb{S}^r$, then the PCW bound reduces to the Mori–Tanaka scheme $\mathbb{A}_{PCW}^r = \mathbb{A}_{MT}^r$. In like manner, the dilute scheme is obtained from the PCW bound for $\mathbb{S}_d = \mathbf{0}$.

2.2. Damage evolution and rate form of the constitutive damage law

In case of closed cracks, damage does not evolve. However, for open cracks the damage yield function is built by considering the thermodynamical force \mathcal{F}^{d^r} associated to each d^r (obtained as the negative of the derivative of Ψ with respect to d^r):

$$\mathcal{F}^{d^r} = -\frac{\partial \Psi}{\partial d^r} = -\left(\frac{1}{2}\mathbf{E} + \boldsymbol{\sigma}_0 : \mathbb{C}^{s^{-1}}\right) : \frac{\partial \mathbb{C}^{hom}}{\partial d^r} : \mathbf{E}. \tag{9}$$

A simple damage criterion is considered and defined as:

$$f^r(\mathcal{F}^{d^r}, d^r) = \mathcal{F}^{d^r} - \mathcal{R}(d^r) \leq 0 \tag{10}$$

where $\mathcal{R}(d^r) = h_0(1 + \eta d^r)$ is the local resistance to the damage propagation related to an envelope of critical energy release rate of the materials (or fracture energy) as proposed in [14,15]. h_0 corresponds to the initial damage threshold value, and η represents damage hardening.

The damage evolution law, obtained by assuming a damage normality rule $\dot{f}^r = 0$, reads:

$$\dot{d}^r = \frac{\frac{\partial \mathcal{F}^{d^r}}{\partial \mathbf{E}}}{h_0 \eta - \frac{\partial \mathcal{F}^{d^r}}{\partial d^r}} : \dot{\mathbf{E}} \tag{11}$$

with:

$$\frac{\partial \mathcal{F}^{d^r}}{\partial d^r} = -\left(\frac{1}{2}\mathbf{E} + \boldsymbol{\sigma}_0 : \mathbb{C}^{s^{-1}}\right) : \frac{\partial^2 \mathbb{C}^{hom}}{\partial d^{r^2}} : \mathbf{E} \tag{12}$$

$$\frac{\partial \mathcal{F}^{d^r}}{\partial \mathbf{E}} = -\left(\mathbf{E} + \boldsymbol{\sigma}_0 : \mathbb{C}^{s^{-1}}\right) : \frac{\partial \mathbb{C}^{hom}}{\partial d^r}. \tag{13}$$

Notice that the condition for the stability of damage increasing imposes that $h_0 \eta > 0$ (cf. [16,17]).

The resulting rate form of the constitutive damage law is:

$$\dot{\boldsymbol{\Sigma}} = \mathbb{C}_t^{hom} : \dot{\mathbf{E}} \tag{14}$$

with

$$\mathbb{C}_t^{hom} = \mathbb{C}^{hom} - \sum_{r=1}^N H^r \frac{\left[\left(\mathbf{E} + \boldsymbol{\sigma}_0 : \mathbb{C}^{s^{-1}}\right) : \frac{\partial \mathbb{C}^{hom}}{\partial d^r}\right] \otimes \left[\left(\mathbf{E} + \boldsymbol{\sigma}_0 : \mathbb{C}^{s^{-1}}\right) : \frac{\partial \mathbb{C}^{hom}}{\partial d^r}\right]}{h_0 \eta + \left(\frac{1}{2}\mathbf{E} + \boldsymbol{\sigma}_0 : \mathbb{C}^{s^{-1}}\right) : \frac{\partial^2 \mathbb{C}^{hom}}{\partial d^{r^2}} : \mathbf{E}} \tag{15}$$

where

$$H^r = \begin{cases} 0 & \text{if } f^r < 0 \text{ or if } f^r = 0 \text{ and } \dot{f}^r < 0 \\ 1 & \text{if } f^r = 0 \text{ and } \dot{f}^r = 0. \end{cases} \tag{16}$$

It is convenient to precise that N refers only to open cracks. The criterion which controls crack state (open or close) depends on stress state as:

$$\beta^r = (\boldsymbol{\Sigma} - \boldsymbol{\sigma}_0) : (\underline{n}^r \otimes \underline{n}^r) \tag{17}$$

in which \underline{n}^r is the normal of the r th crack family. Cracks are open when $\beta^r > 0$.

2.3. Numerical modeling of micromechanical model

This study of progressive damage evolution in brittle materials is governed by three main steps: the choice of state variables representing damage (i.e. d^r), the formulation of thermodynamic potential (Eq. (3)) and finally the definition of damage criteria and damage evolution laws (Eqs. (10) and (11)). In the case of discrete microcracking (with N well-known crack families), the micromechanical law does not require any specificity and follows the previous developments. However, in the case of an infinity of crack families on one *rev*, numerical integration on a unit sphere, representing the normal orientations of cracks, is necessary.

Numerical integration on a unit sphere consists of a Gauss integration for which damage is defined by \mathcal{P} variables as: $\underline{d} = \{d^i, i = 1, \dots, \mathcal{P}\}$. \mathcal{P} is the number of integration points (or the number of elements $d\mathcal{S}$ on the sphere); d^i is the damage variable or crack density on the i th $d\mathcal{S}$ angle zone of the unit sphere. Then, macroscopic variables defined from microscopic

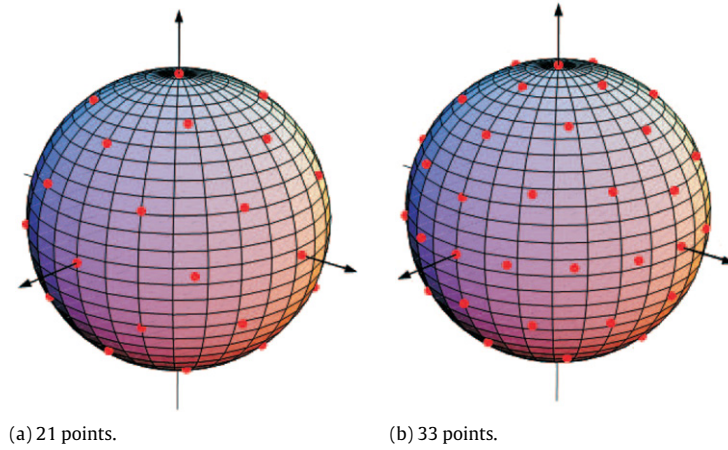


Fig. 1. Repartition of integration points on a sphere following Bazant and Oh microplane approach based on 21 and 33 integration points [21].

ones require weight ϖ^i and orientations \underline{n}^i of each element $d\mathcal{S}^i$ on the sphere. For instance, the following integral which characterizes the above micromechanical model is approximated by:

$$\frac{1}{4\pi} \int_{\mathcal{S}} d(\underline{n})(\underline{n} \otimes \underline{n})d\mathcal{S} = \sum_{i=1}^{\mathcal{P}} \varpi^i d^i \underline{n}^i \otimes \underline{n}^i. \quad (18)$$

In this context, macroscopic deformation as well as all damage variables d^i represent the state variable of the damage model. Macroscopic free energy can then be written through the following symbolic formulation:

$$\Psi = \Psi(\mathbf{E}, \underline{d}) = \Psi(\mathbf{E}, d^1, d^2, \dots, d^{\mathcal{P}}) \quad (19)$$

which can be interpreted as the following weighted sum of all integration domain contributions of \mathcal{P} cracks:

$$\Psi = \frac{1}{2} \mathbf{E} : \mathbb{C}^s : \left(\mathbb{I} - \frac{4\pi}{3} \sum_{i=1}^{\mathcal{P}} w_i d^i \mathbb{A}^i \right) : \mathbf{E} + \sigma_0 : \left(\mathbb{I} - \frac{4\pi}{3} \sum_{i=1}^{\mathcal{P}} w_i d^i \mathbb{A}^i \right) : \mathbf{E}. \quad (20)$$

This numerical integration can be solved by the well-known techniques developed for microplane models in which 21, 33, 37 or 61 points are considered on a half-sphere (see for instance Fig. 1 and [18,19]). Directions and weights of integration come from [20] and are given by Bazant and Oh [18]. They provide the exact integration of high order polynomial functions (e.g. 13° polynomial functions with 61 integration points).

However, one important question is the choice of integration point number. Pensée [22] shows that uniaxial traction or compression test modeling can be performed by the microplane integration approach. Results obtained by schemes based on 21, 33 or 37 points are similar. But Badel [23] observes that the microplane integration approach has an effect on numerical modeling of concrete structures. Even with 61 integration points, results are dispersed meaning that the original Bazant and Oh microplane integration model is unadapted and needs to be extended by considering an alternative approach [24]. These discussions put in evidence the difficulties of the approach. The choice of integration scheme is a largely open question and has to be considered in the following for tunnel excavation modeling in argillite (Section 3).

2.4. Integration in a finite element code of the micromechanical model

Based on the developments proposed previously, the micromechanical model of damage is implemented in the finite element code LAGAMINE from the Université de Liège. The algorithm of local integration is based on the following approach:

1. State variables initialization:

$$\begin{cases} \mathbf{E}_{j+1} = \mathbf{E}_j + \Delta \mathbf{E}_{j+1} \\ d_{j+1}^r = d_j^r \quad r = 1, \dots, \mathcal{P}. \end{cases}$$

2. Checking of damage criteria f^r (Eq. (10)).
3. Calculation of damage increment for each r -crack family:

$$\Delta d_{j+1}^r = \frac{f^r}{h_0 \eta - \frac{\partial \mathcal{F}^d}{\partial d}}.$$

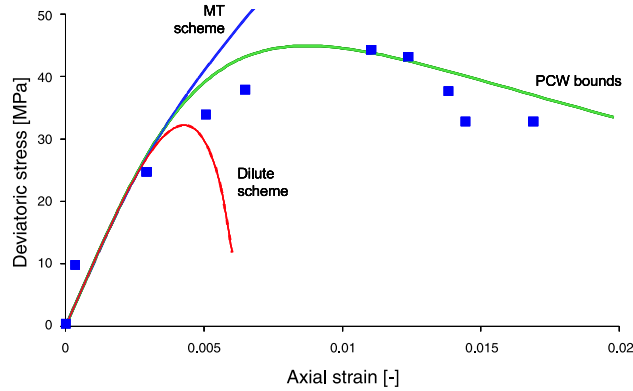


Fig. 2. Calibration of triaxial compression test under 15 MPa confining pressure on Opalinus Clay (□) by dilute scheme, Mori–Tanaka scheme and PCW bounds.

4. Determination of new damage state variables:

$$d_{j+1}^r = d_j^r + \Delta d_{j+1}^r \quad r = 1, \dots, \mathcal{P}.$$

5. Calculation of the new macroscopic stress tensor:

$$\Sigma_{j+1} = \mathbb{C}_{j+1}^{hom}(d_{j+1}) : (\mathbf{E}_{j+1} + \sigma_0 : \mathbb{C}^{s-1}).$$

6. Prediction of each crack state (open or close) for the following step $j + 2$:

$$\beta_{j+2}^r = (\Sigma_{j+1} - \sigma_0) : (\underline{n}^r \otimes \underline{n}^r).$$

3. Applications to tunnel excavation modeling in argillite

3.1. Position of the problem

In the context of nuclear waste storage disposal, we are interested in modeling the behavior of deep geological layers like argillite (Callovo–Oxfordian Clay in France – Bure and Opalinus Clay in Switzerland – Mont Terri, for instance). These rocks are initially very compacted, with low permeability and few microcracks. However, drilling the storage disposal perturbs these materials by modifying rock properties in the tunnel surrounding area. Depending on the resistance of the rock and the depth of the tunnel, micro- or macrocracks are created and can grow in the so-called *Excavation Damaged Zone* (EDZ).

To characterize this phenomena, we propose to study a tunnel excavation in argillite by using the above micromechanical approach. For instance, we have chosen an argillite which refers to Opalinus Clay. According to the literature (see for instance [25,26]), the Young modulus and Poisson ratio can be respectively estimated to be $E = 10$ MPa and $\nu = 0.24$. Damage parameter values of equation Eq. (10) are estimated thanks to a triaxial compression test calibration (see Fig. 2). This triaxial test, described in [27], is performed under 15 MPa confining pressure. Trial and error calibrations provide the stress–strain curve fittings presented in Fig. 2 on which for the three homogenization schemes $h_0 = 100$ J/m² and $\eta = 2500$. These curves show that the dilute scheme is at the origin of a too brittle homogenized behavior, whereas the Mori–Tanaka scheme generates a too hardened one. Only PCW bounds well estimate the stress–strain curve peak and the Opalinus Clay softening regime. This last one is then the only one used in the following to model tunnel drilling.

3.2. Numerical modeling of tunnel excavation

The synthetic tunnel case considered is inspired from the SELFRAC experiment [1,5] with a 5 cm tunnel radius. Its excavation is numerically performed by reducing the stress state from an initial stress value (equal to 5.6 MPa, which is close to the initial stress state in the Mont Terri Underground Research Laboratory (URL) where Opalinus Clay is studied) to 0 MPa on one border representing the future tunnel wall.

To put in evidence the EDZ, damage is characterized by a scalar variable d resulting from numerical integration of all damage variables d^r as follows:

$$d = \sum_{r=1}^{\mathcal{P}} \varpi^r d^r \tag{21}$$

in which \mathcal{P} corresponds to the number of integration points associated to crack families and ϖ^r coefficients are the integration point weights. To perform this integration, we first propose to consider the Bazant and Oh microplane approach [18].

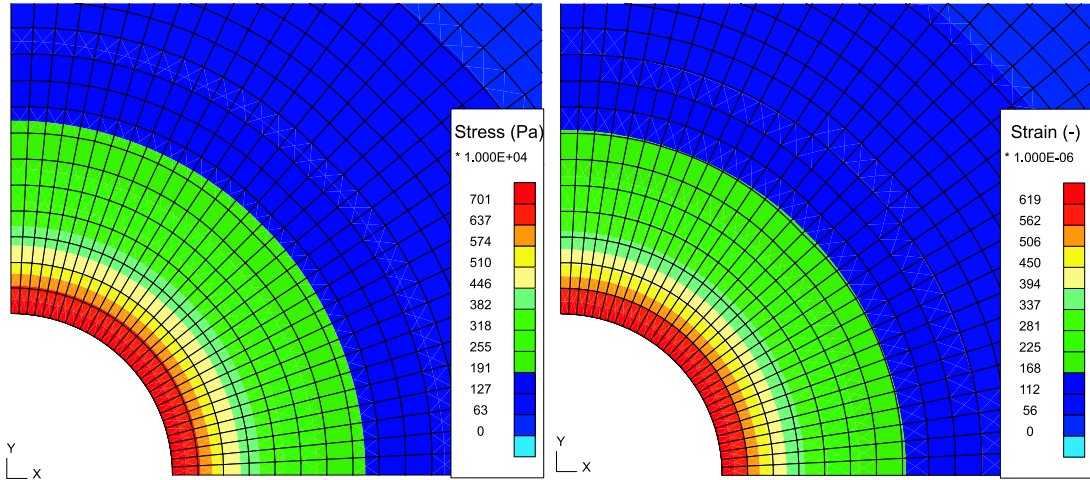


Fig. 3. Repartition of equivalent von Mises stress and strain fields around tunnel after excavation following a microplane model based on 21 integration points on a half-sphere.

3.2.1. *Micromechanical modeling with Bazant and Oh microplane approach*

In the micromechanical model defined in Section 2, the integrated equations are discretized by microplane models. Due to the absence of data concerning the nature and the number of the initial microcracking, a randomly oriented distribution of microcracks is assumed. As a first approximation, the Bazant and Oh microplane approach [18] is considered. This numerical integration procedure is inspired from studies on microplane models following the well-known Gaussian scheme. In this method, integration formulation is determined from a system of linear algebraic equations representing the conditions of the three dimensional Taylor series expansion of the integrated function. It consists of defining, at each material point r , facets or microplanes representing all the possible orientations \underline{n}^r on a unit radius hemisphere (due to symmetry). These orientations are weighted by the facet surface coefficients ϖ^r . Then, on a half-sphere, Bazant and Oh [18] have defined an integration scheme based on 21, 33, 37 or 61 integration points.

Modeling tunnel drilling in this way provides results presented on Figs. 3 and 4 corresponding to von Mises equivalent stress and strain fields and the damage field around the tunnel after excavation. The von Mises equivalent stress and strain fields are respectively given by:

$$\Sigma_{eq} = \sqrt{\frac{1}{2} \hat{\Sigma}_{ij} \hat{\Sigma}_{ij}} \quad \text{and} \quad E_{eq} = \sqrt{\frac{2}{3} \hat{E}_{ij} \hat{E}_{ij}} \tag{22}$$

in which $\hat{\Sigma}$ corresponds to the deviatoric stress and similarly $\hat{E}_{ij} = E_{ij} - \bar{E}$ with \bar{E} the average strain.

Material parameters, initial stress state and excavation processes are isotropic, therefore stress, strain and damage fields should also be isotropic and their repartitions around the excavated zone should describe a regular ring. Although this is the case for stress and strain fields (see Fig. 3), the damage field shows some fluctuations around the tunnel: damage evolution on different cross sections around the excavation are not exactly the same as shown in Fig. 4. These fluctuations exist whatever the number of integration points considered on a half-sphere is (21, 33 or 61—see Fig. 5). However, the most important fluctuations are observed for the smallest number of integration points and fluctuations are smoothed when integration point number increases.

Even if Opalinus Clay behavior presents a softening regime, fluctuations should not be due to strain localizations. It seems to be explained by numerical instabilities due to a too strong damage variable sensitivity in this kind of geotechnical problem. In fact, during tunnel excavation, we expect that at the beginning of the unloading process the behavior function is quite smooth. But at later stages, it should exhibit sharp or localized variations, which are difficult to represent in the form of polynomials, even of high order. It means that the previous Gaussian scheme is unadapted to approximate damage evolution around tunnel excavation. Notice that no instabilities were observed previously during triaxial compression test modeling in Fig. 2, the Opalinus Clay behavior under triaxial loading is easily approximated by a polynomial function.

To try to keep the damage field around the tunnel stable (isotropic), another integration model is introduced in the following by considering the Badel and Leblond [24] alternative scheme.

3.2.2. *Micromechanical modeling with Badel and Leblond integration scheme*

Qiu and Crouch [28] have already observed that numerical modeling with the help of numerical integration is not simple. For instance, they found that convergence of the results is not guaranteed when modeling compression tests. Reaching convergence is more difficult for the axial stress – volumetric strain curve, especially in the post-peak range, than for the axial stress–axial strain curve. Furthermore, it seems that the simple strategy consisting of increasing the number of

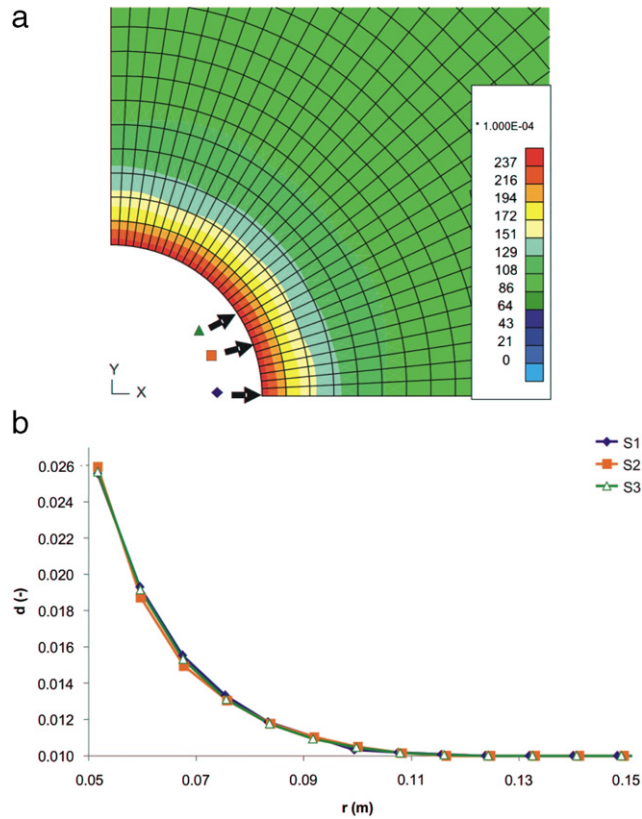


Fig. 4. Repartition of damage variable around tunnel after excavation following a microplane model based on 21 integration points on a half-sphere (a) and evolution on three cross sections (b).

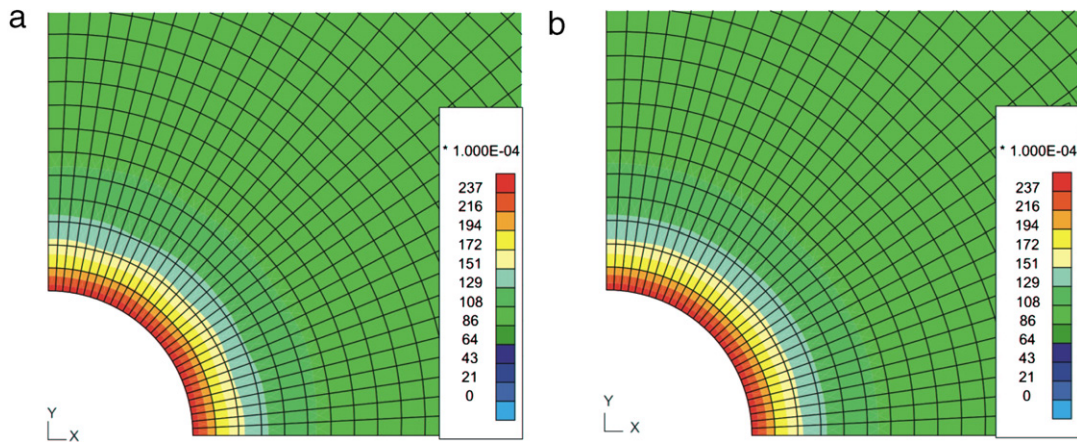


Fig. 5. Repartition of damage variable around tunnel after excavation following a microplane model based on 33 (a) and 61 (b) integration points on a half-sphere.

Gauss points does not appear to be optimal. Generating a high-order Gaussian integration scheme is a cumbersome task. Then, Badel and Leblond [24] have proposed to improve the Bazant and Oh microplane integration scheme by developing an automatic strategy as follows. In their approach, numerical integration of a function is based on a subdivision of the integration interval into many sub-intervals. It consists of meshing a hemisphere by an automatic refinement. Starting from a regular semi-dodecahedron with six pentagonal faces, each pentagon is divided into five equal isosceles triangles. The center of the pentagon is radially projected onto the hemisphere. Each triangle can next be divided into four equal triangles, for which the triangle apex is also radially projected onto the hemisphere. The integral of any function over any triangle is approximated by its value at the centroid of the triangle, the integration point orientation projected onto the hemisphere,

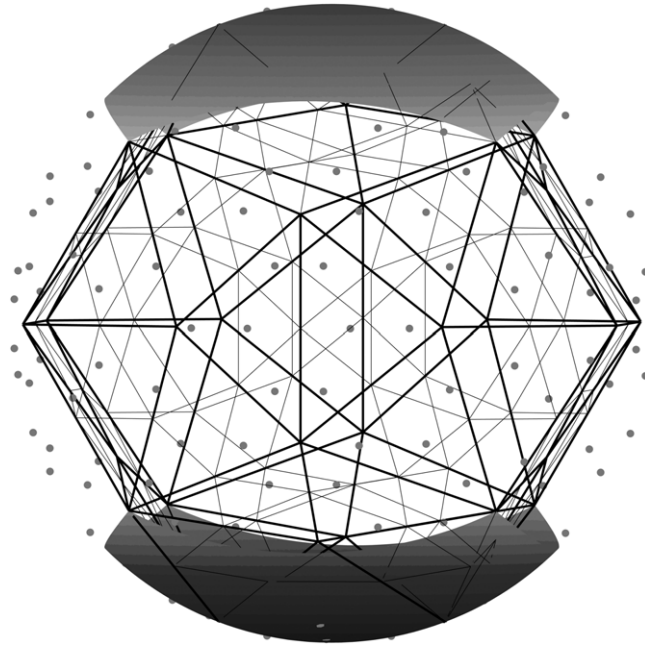


Fig. 6. Repartition of integration points on sphere following the Badel and Leblond approach from triangle meshing of pentagonal faces included inside the sphere (symbolized by the gray zones).

and weighted by its area (see one illustration on Fig. 6 in the case of 120 integration points on a half-sphere). The global integral over the hemisphere is obtained by the sum of such elementary integrals. A big advantage in this approach is that this process can be iterated indefinitely.

Applying this method to the modeling of a tunnel excavation provides an isotropic damage field around the tunnel. In fact, Fig. 7 shows that using this new integration scheme with 120 integration points permits us to stabilize the damage response around the tunnel. The numerical result is stable on each cross section considered. Then, it seems that the Badel and Leblond integration scheme permits us to obtain a better numerical efficiency in the case of this complex geotechnical problem thanks to a good numerical approximation of rock damaged behavior. Furthermore, one can notice that the EDZ predicted by the above results has a size equal to the tunnel radius and damage strongly decreases from the tunnel wall to the limit of the EDZ. These observations seem realistic and correspond to fractures occurring during unloading as commonly observed in Mont Terri URL [25]. The solved damage problem is then both physically and numerically satisfying.

4. Conclusion

The present study concerns the use of a micro–macro approach to model geotechnical problems as the tunnel excavation process in argillite. To this end, we have proposed a homogenization-based formulation accounting for initial stresses. This model is applied to characterize the Opalinus Clay behavior, which is a well-known clayey rock studied in the context of radioactive nuclear waste storage. It shows that numerical considerations need to be carefully taken into account in order to describe accurately the material behavior and the induced damage with the finite element method. More particularly, the integration scheme of the micromechanical model plays an important role and can be conducive to numerical instabilities. In fact through a simple application on tunnel drilling, it has been shown that the distribution of damage evolution around the tunnel is difficult to represent by an integration method based on a polynomial approximation which is derived from microplanes (even of high order of the Bazant and Oh microplane theory [18]). It means that such a Gaussian scheme seems to be unadapted to the numerical integration of damage around the tunnel. Then, we have proposed to switch to the alternative integration scheme proposed in [24]. This one has permitted us to obtain a better numerical efficiency, allowing the advantage of an easier refinement than the Bazant and Oh approach if necessary. Unfortunately, the price to pay is an increase of the number of integration points (120 points seems necessary to well converge in the proposed problem), imposing an increase of the number of state variables that need to be stored and updated at each loading step. Nevertheless this could be avoided by taking advantage of the adaptative mesh refinement capability of the Badel and Leblond approach. The scheme and the associated number of integration points can be refined at different stages of loading (as already proposed by Qiu and Crouch [28]). Then, at the beginning of loading when the behavior curve is quite smooth, it is possible to start with a small number of integration points. At later stages, when the behavior curve shows localized variations, the number of integration points is increased to be automatically adapted to the degree of the approximate polynomial which guarantees good convergence.

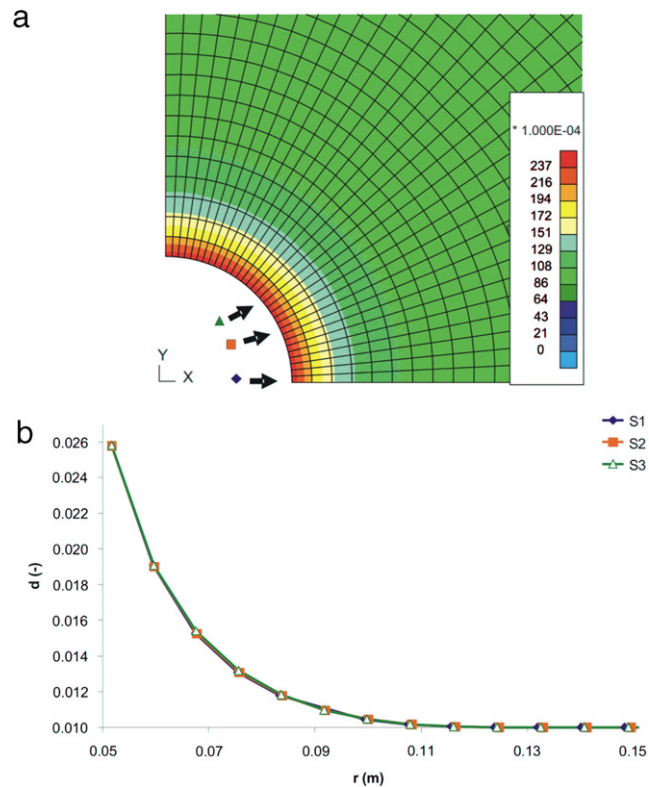


Fig. 7. Repartition of damage variable around tunnel after excavation following a microplane model based on 120 integration points on a half-sphere (a) and evolution on three cross sections (b).

Acknowledgments

The authors would like to thank the F.R.S.-FNRS, the national funds of scientific research in Belgium, for their financial support of the FRFC project.

References

- [1] F. Bernier, X.L. Li, W. Bastiaens, L. Ortiz, M. Van Geet, L. Wouters, B. Frieg, P. Blumling, J. Desrues, G. Viaggiani, C. Coll, S. Chanchole, V. De Greef, R. Hamza, L. Malinsky, A. Vervoort, Y. Vanbrabant, B. Debecker, J. Verstraelen, A. Govaerts, M. Wevers, V. Labiouse, S. Escoffier, J.F. Mathier, L. Gastaldo, Ch. Bühler, Fractures and self-healing within the excavation disturbed zone in clays (selfrac), Final report, 5th EURATOM Framework Programme (1998–2002), 2007.
- [2] Y. Jia, H.B. Bian, G. Duveau, K. Su, J.F. Shao, Hydromechanical modelling of shaft excavation in Meuse/Haute-Marne laboratory, *Phys. Chem. Earth* 33 (2008) 422–435.
- [3] Q.Z. Zhu, D. Kondo, J.F. Shao, Micromechanical analysis of coupling between anisotropic damage and friction in quasi brittle materials: role of the homogenization scheme, *Int. J. Solids Struct.* 45 (2008) 1385–1405.
- [4] L. Dormieux, D. Kondo, F.-J. Ulm, *Microporomechanics*, Wiley, 2006.
- [5] S. Levasseur, R. Charlier, B. Frieg, F. Collin, Hydro-mechanical modelling of the excavation damaged zone around an underground excavation at Mont Terri rock laboratory, *Int. J. Rock Mech. Min. Sci.* 47 (3) (2010) 414–425.
- [6] S. Levasseur, F. Collin, R. Charlier, D. Kondo, On a class of micromechanical damage models with initial stresses for geomaterials, *Mech. Res. Commun.* 37 (2010) 38–41.
- [7] S. Levasseur, F. Collin, R. Charlier, D. Kondo, A two scale anisotropic damage model accounting for initial stresses in microcracked materials, *Eng. Fracture Mech.* 78 (2011) 1945–1956.
- [8] S. Levasseur, F. Collin, R. Charlier, D. Kondo, A micro-macro approach of permeability evolution in rocks excavation damaged zones, *Computers and Geotechnics* (submitted for publication).
- [9] N. Laws, On the thermostatics of composite materials, *J. Mech. Phys. Solids* 21 (1973) 9–17.
- [10] V.M. Levin, Thermal expansion coefficient of heterogeneous materials, *Mekh. Tverd. Tela* 2 (1967) 83–94.
- [11] L. Dormieux, D. Kondo, Poroelasticity and damage theory for cracked media, in: L. Dormieux, F.J. Ulm (Eds.), *Applied Micromechanics of Porous Media*, CISM, 2005, pp. 153–183.
- [12] T. Mura, *Micromechanics of defects in solids*, second ed., Martinus Nijhoff Publ., 1987.
- [13] P. Ponte-Castaneda, J.R. Willis, The effect of spatial distribution on the effective behavior of composite materials and cracked media, *J. Mech. Phys. Solids* 43 (12) (1995) 1919–1951.
- [14] J.-J. Marigo, Formulation of a damage law for an elastic material, *Académie des Sciences (Paris), Comptes Rendus, Serie II-Mécanique, Physique, Chimie, Sciences de l'Univers, Sciences de la Terre* 292 (19) (1981) 1309–1312.
- [15] Ch. Ouyang, B. Mobasher, S.P. Shah, An r-curve approach for fracture of quasi-brittle materials, *Eng. Fract. Mech.* 37 (1990) 901–913.
- [16] S. Andrieux, Y. Bamberger, J.-J. Marigo, Un modèle de matériaux microfissuré pour les roches et les bétons, *J. Méca. Théor. Appl.* 5 (1986) 471–513.

- [17] L. Dormieux, D. Kondo, Micromechanics of damage propagation in fluid-saturated cracked media, *Revue Européenne de Génie Civil* 11 (7–8) (2007) 945–962.
- [18] Z.P. Bazant, B.H. Oh, Efficient numerical integration on the surface of a sphere, *Z.A.M.M.* 66 (1986) 37–49.
- [19] I. Carol, P. Prat, Z.P. Bazant, New explicit microplane model for concrete: theoretical aspects and numerical implementation, *Int. J. Solids Struct.* 29 (1992) 1173–1191.
- [20] A.H. Stroud, *Approximate calculation of multiple integrals*, Prentice Hall, Englewood Cliffs, New Jersey, 1971.
- [21] Q. Zhu, *Applications des approches d'homogénéisation à la modélisation tridimensionnelle de l'endommagement des matériaux quasi fragiles : formulations, validations et implémentations numériques*, Ph.D. Thesis, Université des Sciences et Technologies de Lille, 2006.
- [22] V. Pensée, *Contribution de la micromécanique à la modélisation tridimensionnelle de l'endommagement par mésosfissuration*, Ph.D. Thesis, Université des Sciences et Technologies de Lille, 2002.
- [23] P. Badel, *Contributions à la simulation numérique de structures en béton armé*, Ph.D. Thesis, Université Paris 6, 2001.
- [24] P.-B. Badel, J.-B. Leblond, A note on integration schemes for the microplane model of the mechanical behaviour of concrete, *Comm. Num. Methods Eng.* 20 (2004) 75–81.
- [25] P. Bossart, P.M. Meier, A. Moeri, Th. Trick, J.C. Mayor, Geological and hydraulic characterization of the excavation disturbed zone in the opalinus clay of the mont terri rock laboratory, *Eng. Geology* 66 (2002) 19–38.
- [26] C.D. Martin, G.W. Lanyon, Measurement of in situ stress in weak rocks at mont terri rock laboratory, Switzerland, *Int. J. Rock Mech. Mining Sci.* 40 (7–8) (2003) 1077–1088.
- [27] L. Laloui, B. Francois, Benchmark on constitutive modeling of the mechanical behaviour of opalinus clay, Mont terri project, Technical report, NAGRA, 2008.
- [28] Y. Qiu, R.S. Crouch, Spurious compaction in the microplane model and new adaptative framework, in: *Computational Plasticity*, CIMNE, Barcelona, 1997, pp. 493–499.